BIFURCATION ANALYSIS OF THE QI 3-D FOUR-WING CHAOTIC SYSTEM*

Yanxia Sun[a,b], Guoyuan Qi[a], Zenghui Wang[a,c]
Barend Jacobus van Wyk[a]

[a]F'SATIE, Dept. of Electrical Engineering, Tshwane University of Technology
Pretoria 0001, South Africa
[b]Laboratoire Images, Signaux et Systèmes Intelligents
LiSSi, E.A. 3956, Universite Paris-Est, Paris 94010, France
[c]Department of Electrical and Mining Engineering, University of South Africa
Johannesburg 0719, South Africa

(Received November 23, 2009; revised version received January 12, 2010; final version received February 8, 2010)

This paper analyzes the pitchfork and Hopf bifurcations of a new 3-D four-wing quadratic autonomous system proposed by Qi *et al.* The center manifold technique is used to reduce the dimensions of this system. The pitchfork and Hopf bifurcations of the system are theoretically analyzed. The influence of system parameters on other bifurcations are also investigated. The theoretical analysis and simulations demonstrate the rich dynamics of the system.

PACS numbers: 05.45.–a

1. Introduction

Research on bifurcations can benefit many fields such as electricity, communication, information science, medical science, *etc.* Up to now, many positive research results have been achieved [1–5]. Chaotic systems, with complex topological structures and their applications have been studied with increasing interest in recent years. Generalizing Chua's circuit [6] having multi-scroll attractors and generalizing the Lorenz system [7] having double-wing attractors are two examples for this research.

* This work was supported by grants from the Innovative Research Foundation of Tshwane University of Technology, the National Scientific Foundation of China (10772135, 60774088) and the Scientific Foundation of Tianjin City, P.R. China (07JCYBJC05800), the Scientific and Technological Research Foundation of Ministry of Education, P.R. China (207005).

The generation and analysis of four-wing chaotic attractors have been attracting more and more attention. Qi *et al.* found that by adding a quadratic term to a 4-dimensional (4-D) system, the number of equilibrium classification can be increased from 3 to 5, and four-wing attractors can be generated [8–10]. More recently, Qi *et al.* proposed a new 3-D quadratic autonomous system [11], generating a four-wing chaotic attractor with very complicated topological structures over a large range of parameters. The disordered dynamics has been demonstrated by the large positive Lyapunov exponent and the extremely broad frequency bandwidth. However, there is no theoretical analysis about the route to chaos through period-doubling bifurcations, such as the pitchfork and Hopf bifurcations.

The bifurcation analyze for the generalized Lorenz systems with double wings and the generalized Chua systems have been extensively investigated [12]. It is very significant to study pitchfork and Hopf bifurcations of this new 3-D four-wing chaotic attractor to investigate more complex properties. In this paper we discuss the local bifurcations for the Qi 3-D four-wing system. The conditions under which pitchfork and Hopf bifurcations exist are developed in detail by using the center manifold theorem and bifurcation theory. Numerical simulations and mathematical analysis exhibit the rich dynamical characteristics of the system.

2. Pitchfork bifurcation at the origin

The Qi 3-D four-wing system [11] is described as

$$\begin{aligned} \dot{x} &= a(y-x) + eyz\,, \\ \dot{y} &= cx + +dy - xz\,, \\ \dot{z} &= -bz + xy\,, \end{aligned} \tag{1}$$

where a, b, d are all real positive constant parameters and c, e are real constant parameters.

The Jacobian matrix system (1), evaluated at (x^*, y^*, z^*) is

$$J = \begin{bmatrix} -a & a+ez^* & ey^* \\ c-z^* & d & -x^* \\ y^* & x^* & -b \end{bmatrix}. \tag{2}$$

When $c > -d$, the system has five equilibria, when $c < -d$, the system has three equilibria. The equilibrium $S_0 = [0,0,0]$ of system (1) undergoes a pitchfork bifurcation on the hyper-plane where parameters $c = -d$. The characteristic equation at S_0 is

$$f(\lambda) = (\lambda + b)\left(\lambda^2 + (a-d)\lambda - (ad+ac)\right)\,. \tag{3}$$

It is obvious that $-b$ is one of the roots of (3), and the other two roots do not always have negative real parts according to the Routh–Hurwitz condition.

2.1. Analysis on the pitchfork bifurcations

From Eq. (3) with $c = -d$ and $d < a$, we have $\lambda_1 = 0$, $\lambda_2 = d - a < 0$, $\lambda_2 = -b < 0$ and the corresponding eigenvectors

$$v_1 = [1 \quad 1 \quad 0]^T \,, \qquad v_2 = [a \quad d \quad 0]^T \,, \qquad v_3 = [0 \quad 0 \quad 1]^T \,. \tag{4}$$

According to the center manifold theorem [13], let parameter c be the local bifurcation parameter at $-d$, the system (1) could generate pitchfork bifurcation when $\lambda_1 = 0$ and λ_2, $\lambda_3 < 0$. In the following its existence and condition are investigated.

In the domain of $c = -d$, and $d < a$, let $c = -d + \xi$, with ξ sufficiently small. Using the Taylor expansion, we then have

$$\lambda_1 = \frac{d-a}{2} + \frac{1}{2}\sqrt{a^2 + 2ad + d^2 + 4a(-d+\xi)} = \frac{a\xi}{(a-d)} + o\left(\xi^2\right) \,. \tag{5}$$

By utilizing the eigenvectors in Eq. (4) as the basis of new coordinates $(u, v, w)^T$, system (1) becomes

$$\begin{bmatrix} \dot{u} \\ \dot{v} \\ \dot{w} \end{bmatrix} = \begin{bmatrix} 0 & 0 & 0 \\ 0 & (d-a) & 0 \\ 0 & 0 & -b \end{bmatrix} \begin{bmatrix} u \\ v \\ w \end{bmatrix} + \begin{bmatrix} g_1 \\ g_2 \\ g_3 \end{bmatrix} , \tag{6}$$

where

$$\begin{aligned} g_1 &= \frac{1}{d-a}\left((de+a)uw + \left(d^2e + a^2\right)vw\right) , \\ g_2 &= -\frac{1}{d-a}((1+e)uw + (a+ed)vw) , \\ g_3 &= u^2 + (a+d)uv + adv^2 \,. \end{aligned}$$

Because $\lambda_1 = 0$, λ_2, $\lambda_3 < 0$, there exists a center manifold which is tangent to the u axis. The center manifold is expressed as

$$\begin{aligned} W^c(S_0) = \Big\{ &(u, v, w) \in R^3 | v = h_1(u) \,, \qquad w = h_2(u) \,, \\ &|u| < \delta, h_i(0) = 0 \,, \qquad Dh_i(0) = 0 \,, \qquad i = 1, 2 \Big\} \,. \end{aligned} \tag{7}$$

For δ sufficiently small, the center manifold $W^c(S_0)$ can be found. Since $h_i(0) = 0, Dh_i(0) = 0, i = 1, 2$, $h_1(u)$ and $h_2(u)$ can be expressed in these forms

$$\begin{aligned} v &= h_1(u) = a_1u^2 + b_1u^3 + c_1u^4 + \cdots \,, \\ w &= h_2(u) = a_2u^2 + b_2u^3 + c_2u^4 + \cdots \,. \end{aligned} \tag{8}$$

Substituting (8) into (6) and comparing the coefficients of u^2, u^3, u^4, we have

$$\begin{aligned} a_1 &= 0\,, \qquad b_1 = \frac{2}{(d-a)^2 b}\,, \qquad c_1 = 0\,, \\ a_2 &= \frac{1}{b}\,, \qquad b_2 = 0\,, \qquad c_2 = \frac{2\left(a^2 + ade - d^2 e\right) + ab - ad}{(d-a)^2 e^3}\,. \end{aligned} \tag{9}$$

Thus the following center manifold equations are obtained

$$\begin{aligned} v &= h_1(u) = \frac{2}{(d-a)^2 b} u^3 + o\left(u^5\right)\,, \\ w &= h_2(u) = \frac{1}{b} u^2 + \frac{2\left(a^2 + ade - d^2 e\right) + ab - ad}{(d-a)^2 b^3} u^4 + o\left(u^5\right)\,. \end{aligned} \tag{10}$$

Finally, substituting (10) into (6), an 1-dimensional (1-D) reduced vector field

$$\begin{aligned} \dot{u} &= \lambda_1 u + \frac{1-a}{(a+1)b} u^3 + o\left(u^5\right) = \frac{a\xi}{a-d} u + \frac{de+a}{(d-a)b} u^3 + o\left(u^5\right)\,, \\ \dot{\xi} &= 0\,, \end{aligned} \tag{11}$$

is obtained. Eq. (11) can be used to investigate the bifurcation of system (1).

By letting $\dot{u} = f(u,\xi) = 0$, and ignoring the term $o(u^5)$ in Eq. (11), we have

$$\begin{aligned} \frac{\partial f}{\partial \xi}(0,0) &= 0\,, & \frac{\partial^2 f}{\partial u^2}(0,0) &= 0\,, \\ \frac{\partial^2 f}{\partial u \partial \xi}(0,0) &= \frac{a}{a-d} \neq 0\,, & \frac{\partial^3 f}{\partial u^3}(0,0) &= \frac{6(de+a)}{(d-a)b} \neq 0\,. \end{aligned} \tag{12}$$

According to the theorem [13], the equilibrium point $(u,\xi) = (0,0)$ undergoes a pitchfork bifurcation at $u = 0$. Furthermore, let

$$\frac{a\xi}{a-d} u + \frac{de+a}{(d-a)b} u^3 = 0\,, \tag{13}$$

leading to $u_1 = 0, u_{2,3} = \pm\sqrt{\frac{ab\xi}{de+a}}$.

Hence, about the equilibria of Eq. (11), we have

(1) when $\xi < 0$, *i.e.* $c < -d$, the reduced 1-D system Eq. (11) has only one equilibrium at origin $u_1 = 0$ because $u_{2,3}$ are a pair of imaginary numbers;

(2) when $\xi > 0$, *i.e.* $c > -d$ it has three equilibria at $u_1 = 0$, $u_{2,3} = \pm\sqrt{\frac{ab\xi}{de+a}}$, respectively. Furthermore, we have

$$\frac{\partial f(\xi,u)}{\partial u}|_{u=u_1} = \frac{a\xi}{a-d} \quad \begin{cases} >0\,, & \xi>0\,; \\ <0\,, & \xi<0\,. \end{cases} \tag{14}$$

$$\frac{\partial f(\xi,u)}{\partial u}|_{u=u_{2,3}} = \frac{-2a\xi}{a-d} < 0\,, \quad \xi > 0\,. \tag{15}$$

Therefore, when $\xi < 0$, the only equilibrium u_1 of system (11) is a sink. At $\xi = 0$, *i.e.* $c = -d$, system (11) generates a pitchfork bifurcation and the equilibria to increase to three. When $\xi > 0$, the equilibrium u_1 becomes a source, and another two equilibria $u_{2,3}$ are sinks. From Eq. (11), it is seen that the range of ξ changes in accordance with a change in system parameters.

The following theorem for the original system (1) is therefore obtained:

Theorem 1: Under condition $d < a$ and ξ sufficiently small, on the hyper-plane $c = -d$, system (1) undergoes a pitchfork bifurcation at origin $S_0 = [0,0,0]$. For $c = -d + \xi$ and $\xi < 0$, there are three equilibria and S_0 is a sink. For $c = -d + \xi$ and $\xi > 0$, two new equilibria emerge and are sinks while S_0 becomes a source.

2.2. Verification of pitchfork bifurcations

In this section, we present some numerical simulations to verify the mathematical analysis. The stability of equilibrium points are studied near the pitchfork bifurcation point.

Let $a = 16$, $b = 43$, $d = 10$, $e = 4$, the equilibria and stabilities of (11) are shown in Fig. 1 (a), where the arrows represent the flow direction. When $\xi < 0$, the reduced system only has one sink u_1. At $\xi = 0$, the system

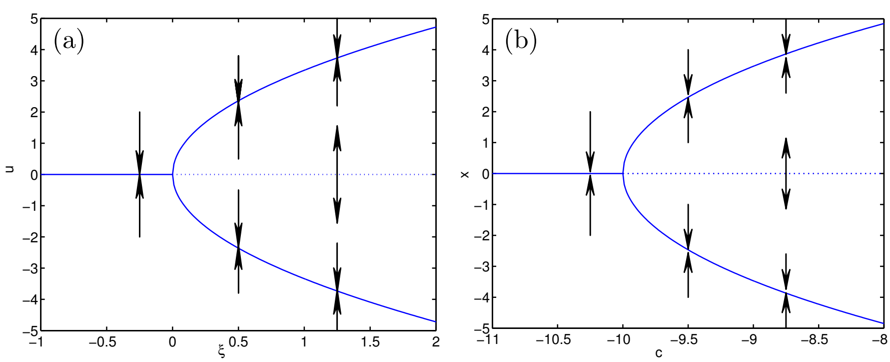

Fig. 1. Pitchfork bifurcation diagram (a) near $\xi = 0$ of system (11); (b) near $c = -d = -10$ of system (1).

undergoes a pitchfork bifurcation and the equilibria increase from one to three. When $\xi > 0$, the equilibrium u_1 becomes a source, and another two equilibria $u_{2,3}$ are sinks. The relationship between system (1) and its reduced center manifold system (11) can be demonstrated in Fig. 1 (a) and Fig. 1 (b). In Fig. 1 (b), parameter $d = 10$ is fixed, and $c = -d + \xi$ changes with ξ increasing. As $c < -10$, there is only one sink at the origin. As $c > -10$, S_0 becomes a source equilibrium, and another new two equilibria S_3, S_4 are sinks. To demonstrate the bifurcation evolution more clearly, three equilibria in 3-D are shown in Fig. 2 where equilibria S_1 and S_2 are omitted. The dotted parabola is composed of the new two stable equilibria S_3, S_4. The equilibria change with an increasing ξ as shown by the arrows. When $\xi \leq 0$, the origin is a sink which can be seen from the system orbit convergence. In the range $\xi \in (0, 2]$, the origin repels the orbits starting around it, so the orbits move away from the origin but are attracted into the upper sink S_3 or lower sink S_4 in terms of initial domains as shown in Fig. 2 where the two orbits converge to the two equilibria of the dotted parabola. The simulation verified Theorem 1.

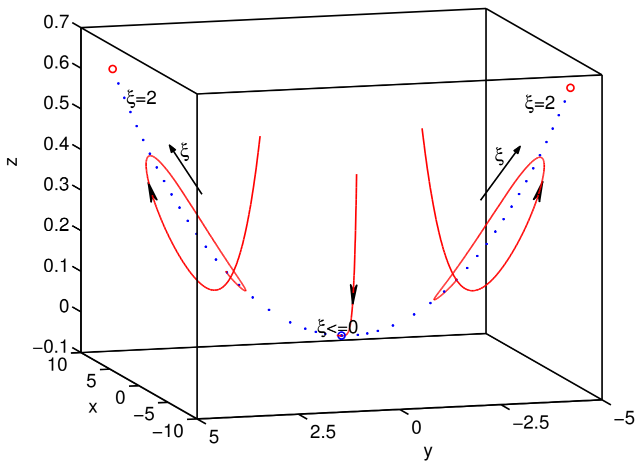

Fig. 2. Pitchfork bifurcation diagram of system (11).

When d is fixed, we analyzed the pitchfork bifurcation above. In fact, the 3-D four-wing system has more complex pitchfork bifurcation on the hyper-plane of $c = -d$. Taking $d \in [0, 10]$, the 3-D pitchfork bifurcation surface generated from Eq. (13), is shown in Fig. 3, which includes the special case at $d = 10$ in Fig. 1 (a). The number of surfaces change from one for $c < -d$ to three for $c > -d$. The blue surfaces are all sinks and the red one all sources. It can be seen that the pitchfork bifurcation is not parabola, but a saddle surface. The bifurcation line is determined by $c = -d$ and $u = 0$.

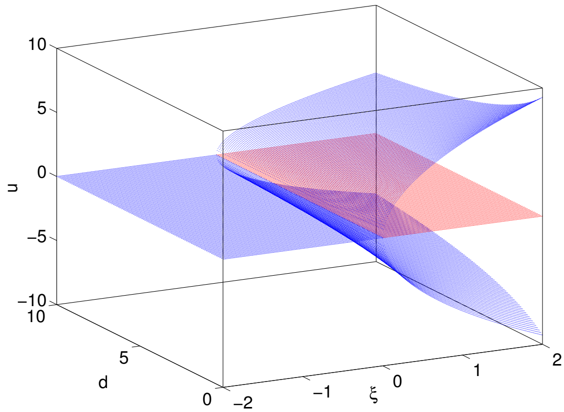

Fig. 3. Pitchfork bifurcation diagram of system (11).

3. Hopf bifurcation of S_0

3.1. Analysis of Hopf bifurcation

In this section, we deal with another kind of bifurcation at the origin $S_0 = [0, 0, 0]$ of system (1) using an analytical method. From Eq. (3), we have the three eigenvalues

$$\lambda_{1,2} = \frac{(d - a \pm \sqrt{a^2 + 2ad + d^2 + 4ac})}{2}\,, \qquad \lambda_3 = -d\,, \tag{16}$$

at the origin. The existence of Hopf bifurcation at a equilibrium is subject to the three following conditions [13]:

(1) There is a pair of imaginary eigenvalues with the rest located on the left half part of s-plane.

(2) Index number $\Lambda \neq 0$.

(3) $\rho_1 = \frac{d\alpha(d)}{dd}|_{d=a} \neq 0$, where $\alpha(d)$ denotes the real part of $\lambda_{1,2}$, d is bifurcation parameter, which means the root loci $\lambda_{1,2}$ must be across the imaginary axis.

Suppose the characteristic equation (3) has pure imaginary roots $\lambda_{1,2} = \pm i\omega$ $(\omega > 0)$. It is easy to show that when $d = d_0 = a$ the Jacobian matrix of system (1) has a pair of imaginary eigenvalues and one negative real eigenvalue, *i.e.*

$$\lambda_{1,2} = \pm i\omega_0\,, \quad \left(\omega_0 = \omega(d_0) = \sqrt{-(a^2 + ac)}\,, (a^2 + ac) < 0\right)\,, \quad \lambda_3 = -b\,, \tag{17}$$

with the corresponding eigenvectors

$$\begin{aligned} v_1 &= \left[\frac{-(-wi+a)}{c}, 1, 0\right]^T, \\ v_2 &= \left[\frac{-(wi+a)}{c}, 1, 0\right]^T, \\ v_3 &= [0, 0, 1]. \end{aligned} \tag{18}$$

By utilizing the real generalized eigenvectors as the basis of new coordinates, system (1) becomes

$$\begin{bmatrix} \dot{x_1} \\ \dot{y_1} \\ \dot{z_1} \end{bmatrix} = \begin{bmatrix} 0 & -\omega & 0 \\ \omega & 0 & 0 \\ 0 & 0 & -b \end{bmatrix} \begin{bmatrix} x_1 \\ y_1 \\ z_1 \end{bmatrix} + \begin{bmatrix} f^1 \\ f^2 \\ f^3 \end{bmatrix}, \tag{19}$$

where

$$\begin{aligned} f^1 &= \frac{1}{c}(wy_1 + dx_1)z_1, \\ f^2 &= -\frac{c^2e + d^2}{cw}x_1z_1 - \frac{d}{c}y_1z_1, \\ f^3 &= -cdw^2x_1^2 - cw^3x_1y_1. \end{aligned}$$

According to the center manifold theorem, there exists a center manifold for Eq. (19), which could be represented locally by

$$\begin{gathered} W^c(S_1) = (x_1, y_1, z_1) \in R^3 | z_1 = h(x_1, y_1), \\ |x_1, y_1| < \delta, \qquad h(0,0) = 0, \qquad Dh(0,0) = 0, \end{gathered} \tag{20}$$

where δ is sufficiently small. We assume that

$$z_1 = h(x_1, y_1) = d_1x_1^2 + d_2x_1y_1 + d_3y_1^2 + d_4x_1^3 + d_5x_1^2y_1 + d_6x_1y_1^2 + d_7y_1^3 + \cdots. \tag{21}$$

The center manifold can be approximately computed by substituting (21) into (19). Comparing the coefficients of the first equation and second equation of (19), we obtain

$$\begin{aligned} d_1 &= \frac{(bc - 2cd)\omega^4 - cdb^2\omega^2}{b\,(b^2 + 4w^2)}, & d_2 &= \frac{-(bc + 2cd)w^3}{b^2 + 4w^2}, \\ d_3 &= \frac{-(bc + 2cd)w^4}{b\,(b^2 + 4w^2)}, & d_4 &= d_5 = d_6 = d_7 = 0. \end{aligned} \tag{22}$$

Therefore, the 3-D vector field is reduced to the following 2-dimensional (2-D) center manifold

$$\begin{bmatrix} \dot{x_1} \\ \dot{y_1} \end{bmatrix} = \begin{bmatrix} 0 & -\omega_0 \\ \omega_0 & 0 \end{bmatrix} \begin{bmatrix} x_1 \\ y_1 \end{bmatrix} + \begin{bmatrix} f^1(x_1, y_1) \\ f^2(x_1, y_1) \end{bmatrix}, \tag{23}$$

where

$$\begin{aligned} f^1(x_1, y_1) &= f^1(x_1, y_1, h(x_1, y_1))\,, \\ f^2(x_1, y_1) &= f^2(x_1, y_1, h(x_1, y_1))\,. \end{aligned} \tag{24}$$

Now we calculate index number Λ by the following formula:

$$\begin{aligned} \Lambda_1 &= \frac{1}{16}\left[f^1_{x_1x_1x_1} + f^1_{x_1y_1y_1} + f^2_{x_1x_1y_1} + f^2_{y_1y_1y_1}\right] \\ &\quad + \frac{1}{16\omega_0}\Big[f^1_{x_1y_1}\left(f^1_{x_1x_1} + f^1_{y_1y_1}\right) \\ &\quad - f^2_{x_1y_1}\left(f^2_{x_1x_1} + f^2_{y_1y_1}\right) - f^1_{x_1x_1}f^2_{x_1x_1} + f^1_{y_1y_1}f^2_{y_1y_1}\Big] \\ &= \frac{1}{16}\left(\frac{\omega^2 - c^2e - d^2}{c\omega}\right)d_2\,. \end{aligned} \tag{25}$$

To meet the condition of index number $\Lambda \neq 0$, we have

$$\omega^2 - c^2e - d^2 \neq 0\,. \tag{26}$$

From Eqs. (17) and (26), we obtain the conditions for the Hopf bifurcation as follows:

$$d = a, a < -c, \omega^2 - c^2e - d^2 \neq 0\,. \tag{27}$$

From Eq. (16), we have

$$\rho_1 = \frac{d\alpha(d)}{dd}|_{d=a} = \frac{1}{2}\,. \tag{28}$$

So under condition (27), a Hopf bifurcation exists at the origin.

Theorem 2: If the parameters of system (1) meet condition (27), system (1) undergoes a Poincare–Anddronov–Hopf bifurcation (Hopf bifurcation) at the origin $S_0 = [0, 0, 0]$. A transition from sink to periodic motion occurs. Moreover, since $\rho_1 = \frac{1}{2} > 0$, the periodic solution emerging after $d > a$, is stable if $\Lambda < 0$, and is unstable if $\Lambda > 0$.

3.2. Simulation of Hopf bifurcation

When $a = 16, b = 43, d = 16, e = -1, c = -18$, we have $\Lambda = -7.5873$ from Eq. (25). According to Theorem 2, a stable periodic orbit emerges from zero equilibrium with $d > a$ in the neighborhood $d = a$. Taking $[0.5, 0.5, 0.5]$ around S_0 as an initial point, when $d = 15.9 < a$, S_0 is sink, as shown in Fig. 4 (a). But when $d = 16.1 > a$, S_0 becomes a stable periodic orbit, as shown in Fig. 4 (b). In the meantime, the zero equilibrium is a source. So we can easily see the transition from the stationary state to the periodic state at the equilibrium point with d changing.

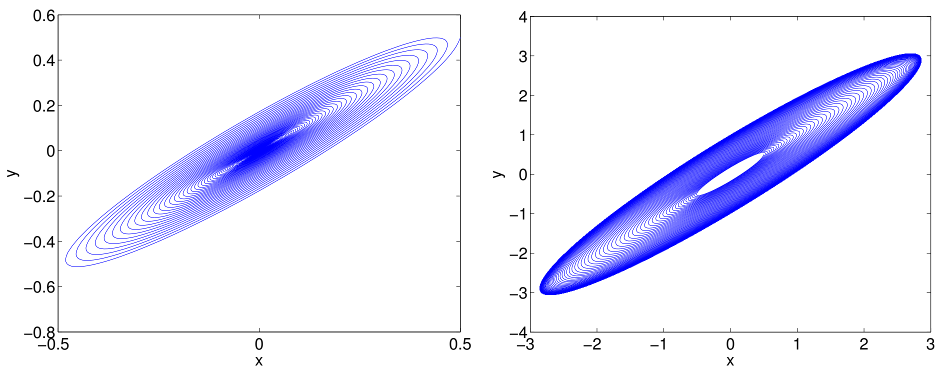

Fig. 4. Hopf bifurcation of system (1) according to theorem 2 (a) $d = 15.9 < a$, the zero equilibrium is a sink, (b) $d = 16.1 > a$, the system orbit is attracted to a stable period orbit in the mean time, the zero equilibrium is a source.

4. Bifurcation analysis related to changes in system parameters

In this section, we investigate how the dynamics of the origin changes with a change of the system parameters. From the characteristic polynomial (3), the polynomial can be written as

$$\lambda^3 + (a + b - d)\lambda^2 + (ab - ad - ac - bd)\lambda - b(ad + ac) = 0\,. \tag{29}$$

To get the marginal stability, the Routh–Hurwits criterion is used, we have

$$\begin{vmatrix} ab - ad - ac - bd & -b(ad + ac) \\ 1 & a + b - d \end{vmatrix} = 0\,. \tag{30}$$

With condition (29), the Hopf number on the bifurcation line [12] is given by

$$\theta = \frac{c_0}{c_2} = \frac{b(ad + ac)}{a + b - d}\,. \tag{31}$$

If θ is given, we can distinguish among the following four different situations:

(1) if θ is real and < 0, the Hopf bifurcation will occur,

(2) if θ is real and > 0, the real Hopf bifurcation will occur,

(3) if θ is undetermined, there is more complex situations (*e.g.* double Hopf),

(4) if $\theta = 0$ the Takens–Boganov point exists.

When $a - d = 0$ is satisfied and $\theta < 0$, the trial steady state undergoes a Hopf bifurcation. For example, when $a = 16$, $b = 43$, $d = 16$, $e = -1$, $c = -18$, we have $a - d = 0$ and $\theta = -32$, which verifies the existence of Hopf bifurcation in Sec. 4. If $a - d \neq 0$ is not satisfied, let $ac + ad - ab + bd - b^2 = 0$ in (30). By submitting this condition into (31) and hence $\theta = b^2$, so $ca + da - ab + bd - b^2 = 0$ and $\theta < 0$ cannot be satisfied simultaneously. The Hopf bifurcation can therefore occur only under the condition $a - d = 0$ and $\theta < 0$.

When $a = 16$, $b = 43$, $c = -16$, $d = 16$, $e = 4$, then $\theta = 0$ and $\lambda_{1,2} = 0$, the trial steady state is a Takens–Boganov (TB) point which is a special of pitchfork bifurcation case. The TB bifurcation indicates the presence of a branch of homoclinic bifurcation.

From (31), when $c > -d$ and $a + b > d$, then $\theta > 0$ and real. The origin undergoes a real Hopf bifurcation, a situation in which two purely real, symmetric eigenvalues are present. The real Hopf situation surface of $ac + ad - ab + bd - b^2 = 0$ plays an important role in formation of the chaotic region and the system in which homoclinic bifurcation exists.

5. Conclusion

In this paper, the pitchfork and Hopf bifurcations of the Qi 3-D four-wing system have been investigated. We have analyzed some basic properties of the system. The stability of fixed points when pitchfork bifurcations occur have been rigorously analyzed from a theoretical point of view. The bifurcation of the period cycle emerging from the zero equilibrium as can be seen from the Hopf bifurcation analysis. Finally, the influence of system parameters on other bifurcations have also been investigated. Using numerical mathematical analysis and simulations, we detected the coexistence of a stable limit cycle and a chaotic attractor which verified rich dynamics of the Qi 3-D four-wing system.

REFERENCES

[1] G. Chen, J. Moiota, H. Wang, *Int. J. Bifur. Chaos* **10**, 511 (2000).

[2] T. Ueta, G. Chen, *Int. J. Bifur. Chaos* **10**, 1917 (2000).

[3] A.Z. Górski, T. Srokowski, *Acta Phys. Pol. B* **37**, 2561 (2006).

[4] X. Wang, L. Tian, *Chaos, Solitions and Fractals* **21**, 193 (2004).

[5] A. Krawiecki, *Acta Phys. Pol. B*, **30**, 2489 (1999).

[6] L.O. Chua, M. Komuro, T. Matsumoto, *IEEE Trans Circuits Syst-I* **48**, 1369 (2001).

[7] G. Chen, J. Lu, *Dynamics of Lorenz System Family: Analysis, Control and Synchronization*, Beijing, Science Press, 2003.

[8] Z. Wang, Y. Sun, B.J. van Wyk, G. Qi, A. van Wyk, *Braz. J. Phys.* **39**, 3 (2009).

[9] G. Qi, G. Chen, Y. Zhang, *Phys. Lett.* **A352**, 386 (2006).

[10] G. Qi, G. Chen, S. Li, Y. Zhang, *Int. J. Bifur. Chaos* **16**, 859 (2006).

[11] G. Qi, G. Chen, *Chaos, Solitions and Fractals* **38**, 705 (2008).

[12] L.F. Mello, M. Messias, D.C. Braga, *Chaos, Solitions and Fractals* **37**, 1244 (2008).

[13] S. Wiggins, *Introduction to Applied Nonlinear Dynamical Systems and Chaos*, 2nd edition, New York, Springer-Verlag, 2003.

[14] G. Thilo, F. Ulrike, *Physica D* **195**, 292 (2004).